

LONG-TERM INSTABILITY OF GPS-BASED TIME TRANSFER AND PROPOSALS FOR IMPROVEMENTS

Z. Jiang¹, D. Matsakis², S. Mitchell², L. Breakiron²,
A. Bauch³, D. Piester³, H. Maeno⁴, and L. G. Bernier⁵

¹Bureau International des Poids et Mesures (BIPM), zjiang@bipm.org

²The United States Naval Observatory (USNO)

³Physikalisch-Technische Bundesanstalt (PTB),
Bundesallee 100, 38116 Braunschweig, Germany

⁴National Institute of Information and Communications Technology (NICT)

⁵Swiss Federal Office of Metrology (METAS)

Abstract

GNSS-based time transfer is the prevalent technique used in the generation of Coordinated Universal Time (UTC); in September 2011, 56 links out of the total of 67 were GNSS-only. These links are realized by combining the data from a single GNSS receiver in each of the time laboratories involved. Some modern receivers have shown only sub-nanosecond variations, but it has been observed that the internal calibration reference of other GPS receivers occasionally jumps by several nanoseconds, and GPS receivers can suffer long-term variations of up to 2 ns per year. In certain situations, without periodic calibrations, these variations can accumulate to form much larger offsets. This would be particularly serious at the PTB, the unique pivot laboratory in the worldwide UTC network, because it would in turn bias the associated subsets of participating laboratories, as well as UTC itself. In this paper, we show the long-term delay instability in the GPS receivers revealed by common-clock and near-zero-baseline observations at METAS, NICT, USNO and PTB. These show phase jumps, seasonal variations, and various forms of linear variations. Based on these findings, we consider how the Type B uncertainty of a link calibration as estimated at a certain epoch can be extrapolated over an extended period so as to estimate the combined uncertainty of [UTC – UTC (k)].

Combining the results of an ensemble of independent GNSS receivers can reduce the influence of individual devices. As a first step, we investigate double-receiver time transfer, and find that the use of a second time-transfer system increases the time stability with regard to measurement noise and receiver phase jumps. Comparison with a third receiver, or use of a completely independent technique such as Two-Way Satellite Time and Frequency Transfer (TWSTFT), helps to identify which receiver has caused an anomaly in the measurements. Such use of an ensemble to monitor individual receiver variations on-site would represent a useful supplement to the BIPM's standard calibrations.

1. INTRODUCTION

Global Navigation Satellite Systems (GNSS) – currently GPS and GLONASS – play the biggest role in time transfer among timing institutes contributing to the realization of Coordinated Universal Time (UTC). In this paper, we consider data collected at the Swiss Federal Office of Metrology (METAS, designated by the acronym CH), the Japanese National Institute of Information and Communications

Technology (NICT), the German Physikalisch-Technische Bundesanstalt (PTB), and the US Naval Observatory (USNO). GNSS time transfer is currently based on individual systems of receiver, antenna, electronics, etc., which for simplicity we shall term “receiver” hereafter. Except for the pivot laboratory PTB, in UTC generation the instabilities of the GNSS receiver systems are indistinguishable from clock variations. If the same GPS receiver were used at the PTB for all UTC links, any miscalibration of a particular laboratory’s receiver, including the PTB’s, would affect solely the evaluation of that laboratory. However, since UTC is generated using not only the PTB’s Two-Way Satellite Time and Frequency Transfer (TWSTFT or TW) links, but also links based on other PTB GNSS receivers, the consequences of one of the PTB receivers varying are more complex. A delay variation of X ns affecting a PTB time transfer system linked to laboratories with a total weight fraction W_X would shift the UTC of those laboratories by $X(1-W_X)$, and shift the UTC of all other laboratories including the PTB by $X W_X$ [1,2]; delay variations in other PTB time transfer systems would have an additive effect whether they were TWSTFT or GNSS.

The instability of GPS receivers has been investigated previously, e.g. [3-12]. Continuous monitoring of their calibrations is not yet feasible, as the absolute calibration of GPS receivers remains both too complex (e.g., requiring the receiver to stop normal operation) and too expensive to be undertaken frequently. Also, at frequencies L1 or L2 [13], the Type B uncertainty published in the BIPM Circular T leads to link uncertainties four times greater than that of any individual receiver. In this study, we compare GPS receivers referenced to a common clock and on near-zero-length baselines. Individual receivers are considered to be independent and the variations/instabilities observed are defined relative to each other. Since the receiver calibration is based on code measurements, the time differences we obtain using GPS P3 data should be similar to those using GPS PPP data because in the PPP solution the phase ambiguities are fixed by a code solution. Only minor systematic differences such as those due to atmospheric effects do not cancel perfectly in common mode.

We categorize the potential long-term instabilities of the GPS receiver systems into three types: 1) constant slope; 2) nanosecond or smaller jumps; 3) quasi-periodic variations.

In the following sections, we first describe the experimental setup, then the results of the numerical analysis, and finally the possible ways of improving the stability of GNSS time transfer. Deeper investigations are needed to better understand the physical causes of changes in the receiver’s internal reference.

2. EXPERIMENTAL SETUP AND DATA

2.1. THE SETUP

Here we define the instability of a receiver as the sum of the instabilities of the indoor receiver itself along with the instabilities of the cables, the splitters, amplifiers, outdoor antenna, and the multipath environment. At present, we can only observe relative variations of the total delay within an ensemble, in which the individual receiver data are reduced to a common clock, as shown in Figure 1.

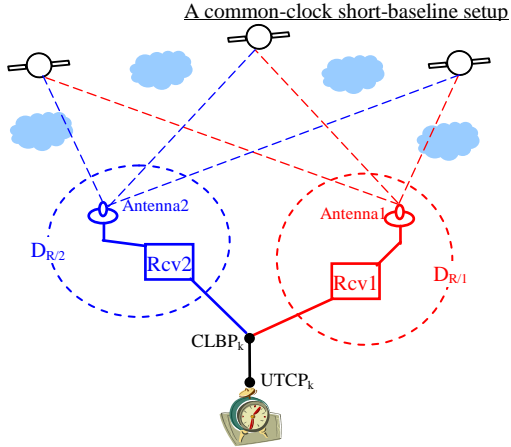


Figure 1. The total delay of a GPS receiver (D_R) at Lab (k) and the common-clock short baseline ($D_{R/2} - D_{R/1}$).

2.2. THE DATA

Data were collected at the laboratories PTB, CH, NICT, and USNO from January 2009 to April 2011 (UTC months 0901 to 1104). Table 1 describes the receivers used in the experiment.

Table 1. Receivers used in the experiment.

Lab.	Receiver system	Type	Link status	Pre-calibration ¹ / ns
PTB ³	PTBB	Ashtech/Z12T	UTC	-
	PTBG	Ashtech/Z12T	backup	-508.65 ± 0.55^2
	PTBT	AOS/TTS3	backup	14.56 ± 0.82
CH	CH01	Ashtech/Z12T	backup ⁴	-
	CH00	POLARX2	backup	7.04 ± 0.21
NICT	NICT A	POLARX2	UTC	-
	NICT B	POLARX2	backup	0.42 ± 0.52
	NICT C	POLARX2	backup	-
USNO	USN3	Ashtech/Z12T	UTC	-
	SPX2	POLARX2	-	-
	NOV1	NovAtel ProPak-V3	backup	-

Notes:

1. The backup receiver calibration with respect to the one regularly used in UTC realization.
2. The number following the symbol \pm is the numerical value of the standard deviation of the calibration comparison, and not a confidence interval.
3. The installation of the PTB receivers PTBB and PTBG was renewed in September-October 2010. Due to the disruption during this period, only data thereafter are studied in this paper.
4. The CH-PTB UTC link is maintained by a TW link.

2.3. DATA REDUCTION

Much of the data analysis was undertaken as part of the BIPM's standard operating procedures, using data that are freely available from the BIPM's anonymous ftp server. Additional RINEX data from some secondary receivers were reduced by the USNO using the sliding-batch PPP procedure to reduce the day boundary discontinuities [14]. The USNO reduction process saves the code and phase residuals of the PPP solutions, because by differencing code residuals from phase residuals, all remaining errors in the clock, orbit, troposphere, and other parameter estimates can be removed. The residuals provide an indication of the noise in the code as well as the greater sensitivity of pseudo-range data to environmental and multipath effects. Since the average code and phase residuals are forced to be zero for any independent PPP solution, the diurnal signature of these errors provides an estimate of the expected seasonal temperature-dependent variations in GPS data. In the sections below, we see how the code-phase residuals of PPP solutions are receiver-dependent. Similar variations are seen in many of the Ashtech receivers, and they are different from the pattern seen in other receiver types. Interestingly, code-phase residuals from CH01 (Ashtech, METAS) and from the Swedish metrology institute SP (JAVAD, Boras, Sweden) show no such effects; great care was taken to minimize the sensitivity of the SP system to multipath and weather. At METAS, the antenna of CH01 (IGS designation is WAB2) is an Ashtech choke-ring antenna with a radome. The antenna cable is an Andrews low-thermal-sensitivity coaxial cable approximately 50 m in length. Only a few meters of the cable lie outdoors; most of the cable is at room temperature inside the building. The roof of the METAS building is large and flat and it is the highest building in the neighborhood. The GPS antennas are mounted above the roof on steel structures 1.5 m high.

In order to better visualize the diurnal signatures in the figures below (Figures 7, 8, 11-13, 16, and 17), a special filter [3] has been applied that maps them into an apparent 10-day periodicity. For every 10-day period shown in the plots, the data are averaged by time of day (modulo integer MJD) to generate a diurnal profile for that 10-day period. The averages are then plotted time-tagged so the first average point is plotted at the MJD of the start of the 10-day period and the last averaged point is plotted as if it were the last point of the 10-day period. The effects of any mismodeling or multipath that only appears at particular hours of the day would also be enhanced. Although the filtering enhances the visibility of the diurnal signature, it should be noted that the figures' implied seasonal delay variations also correspond to seasonal temperature variations. In the case that the temperature difference between summer and winter is 2 to 3 times more than that between night and day, the implied seasonal variations would be at most a nanosecond.

3. LONG-TERM VARIATIONS OF THE RECEIVER CALIBRATIONS

In the analysis, the standard CGGTTS and PPP data were combined to produce hourly or daily data, and these were often smoothed for display so as to better show the longer-term trends.

3.1. CH FOR THE 19-MONTH PERIOD 0910 TO 1104

Figure 2 illustrates the result of a 19-month comparison between CH01 (Ashtech) and CH00 (PolaRx2) for the UTC months 0910-1104. On MJD 55313 (27 April 2010), there was a jump of about 3 ns. Before this and for the first two months after the jump, we note a near constant rate of change of about 0.1 ns per month (about 1.2 ns per year). In total, 14,607 points were compared and the standard deviation was ± 0.423 ns. For the time deviation, we obtain 0.04 ns for an averaging time of 1 hour.

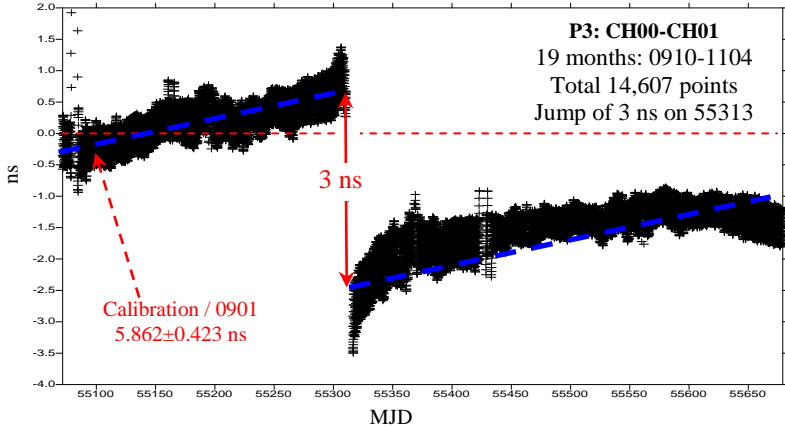


Figure 2. Differences of CH00-CH01 vary between 0910–1104 with an average rate of 0.1 ns per month. A jump of about 3 ns happened on MJD about 55314 (1004). Allowing for this jump would reveal a semi-monotonic 2.0 ns increase from MJD 55100–55650.

The 3 ns jump is coincident with an environmental failure of CH01. As reported by METAS [15], the CH01 receiver originally belonged to a GeTT Station (GeTT for Geodetic Time Transfer [16]), and was operated inside a Peltier-cooled insulated box set at 15 °C. The thermal control of the insulated box failed in April 2010 and the latter was opened to cool down the receiver that would otherwise have overheated. As may be seen in Figure 2, in the months that followed the event, the internal reference of the receiver drifted back slowly by about 1 ns toward its original status, but stabilized after about MJD 55375 without having compensated the total jump of 3 ns. Since the failure, the CH01 receiver has been operated at room temperature (about 22 °C), with the insulated box opened. This permanent change in the ambient temperature may explain the permanent change of about 2 ns in the calibration. An analysis of how carrier-phase software can respond to such jumps was given in Matsakis *et al.* [11]. A PPP analysis of CH00-CH01 performed at METAS [15] shows that the sudden 3 ns jump observed on MJD 55314 is only part of the story. There was a progressive change of calibration before, during the overheating period, and a progressive change of calibration after the insulated box was opened. Figures 3 and 4 show how TWSTFT observations with the PTB can be used to distinguish between variations of CH00 and CH01.

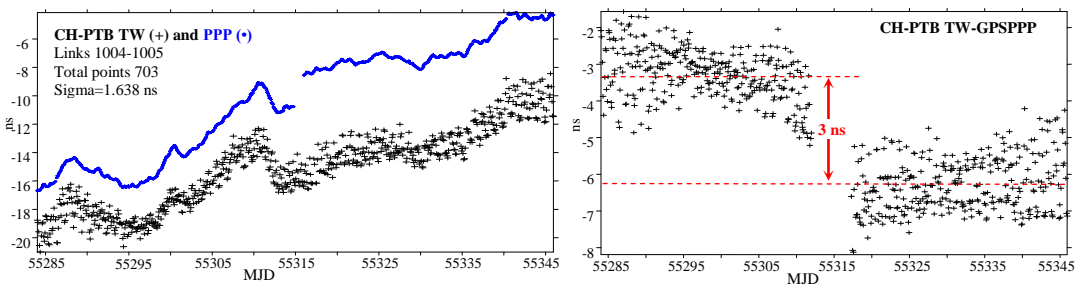


Figure 3. Comparisons between TW link and GPS PPP link. The GPS PPP data were collected from PTB and CH01. *Left:* TW and GPS PPP links; *Right:* TW–GPS PPP. The PPP link is affected by a 3 ns calibration jump due to the GeTT (CH01) failure.

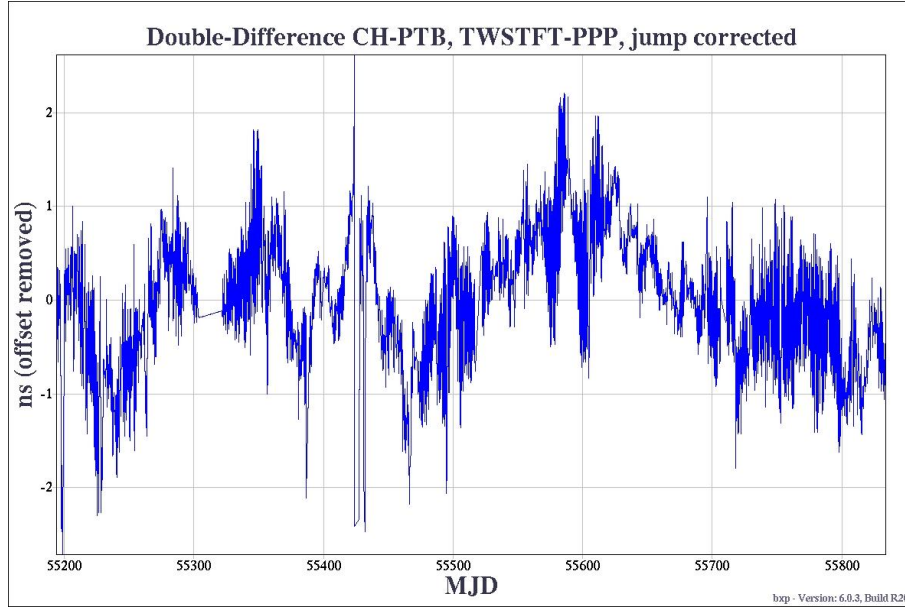


Figure 4. Double-difference between CH01 and PTB linked by TWSTFT and PPP. The 3 ns calibration shift in April, 2010 has been removed. The longer-term fluctuations could be due to either TWSTFT or PPP. However, the long-term stationarity of the curve suggests that the long-term variation of Figure 2 is due to CH00.

3.2. THREE PTB RECEIVERS SINCE 2009

Figures 5 and 6 show the differences between the principal PTB receiver, PTBB, used for PPP and P3 with its backup PTBG, and the multichannel receiver PTBT (which is used for UTC computations with laboratories equipped with GPS C/A and GLN L1C codes). Data were adjusted for calibration shifts when the receivers were moved to a different part of the room between MJD 55461 and 55466. Another correction was made to PTBG data on MJD 55590, when the power supply for the 5 MHz to 20 MHz multiplier that provides the PTBG reference frequency signal was changed. The move to a new location very roughly coincides with the end of the slope in the difference [PTBB – PTBG], although a subnanosecond difference remains, perhaps due to a seasonal effect.

We have no explanation for the irregularities that appear, for example around MJD 55183 (18 December 2009). We analyzed all the available TW and PPP links; however, the data were either incomplete or too noisy, as were data from the PTB's TTS-3 receiver. The heavy snowfall in the month of December 2009 may have caused a problem, as temperature events are known to cause apparently spontaneous and unpredictable calibration jumps in the Ashtech Z12T.

Following the formula in the introduction, any constant or variable bias in the PTB receivers, if not corrected for, would principally affect the Circular T computations of all laboratories linked via the receiver in question, due to their total weight being less than that of the remaining laboratories. Expansion of the plot reveals times of sinusoidal variations of magnitude up to 1.5 ns and periodicity 4-5 days, for example over the last 100 days.

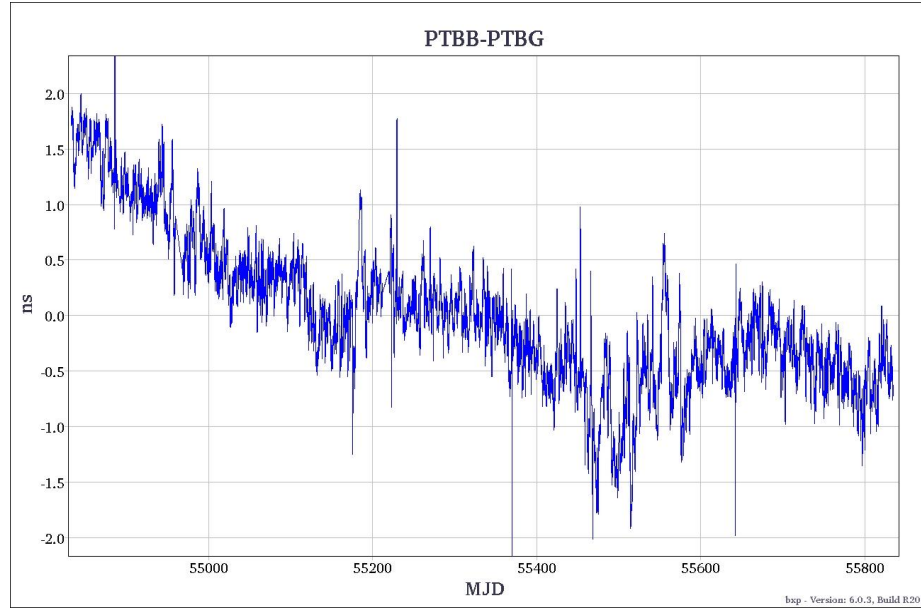


Figure 5. Difference between PPP solutions of PTBB and PTBG, with corrections applied for the minor configuration changes of MJD 55461 and 55466, but not 55488. Although the overall slope seems to have terminated, a sub-nanosecond seasonal variation is still noticeable.

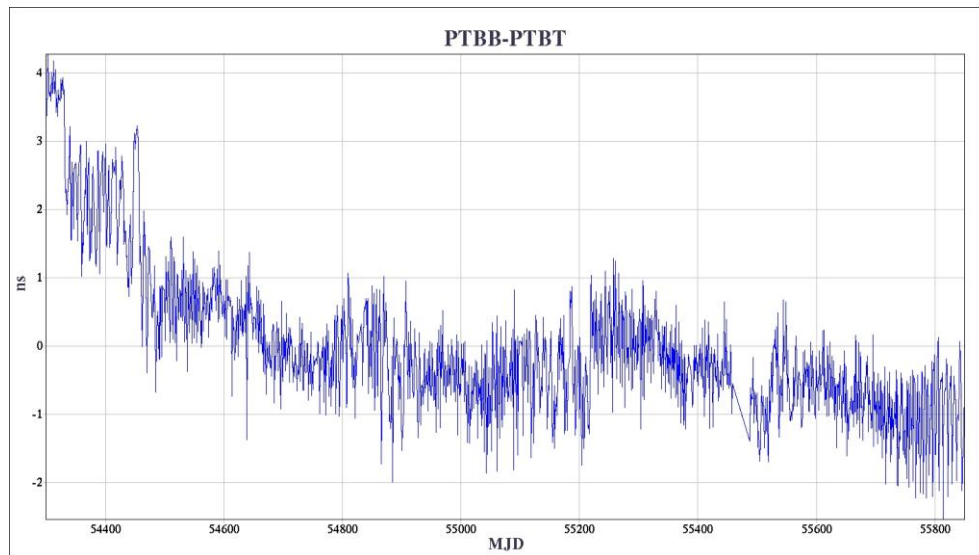


Figure 6. PPP data for the PTBB-PTBT link. The data were shifted slightly for continuity over configuration change 55461-66; zooming into the data reveals that much of the scatter is not white noise. Note that this figure starts at earlier times than the previous figure.

The conclusion that PTBB varied less than PTBG after MJD 55490 is supported in the code-phase residual plots that follow. The motivation behind the figures is provided in Section 2.3; the figures show that the code-phase residuals of PTBG are far more pronounced than for PTBB. This instability in the PTBG's code is probably related to the overall calibration instability of the unit.

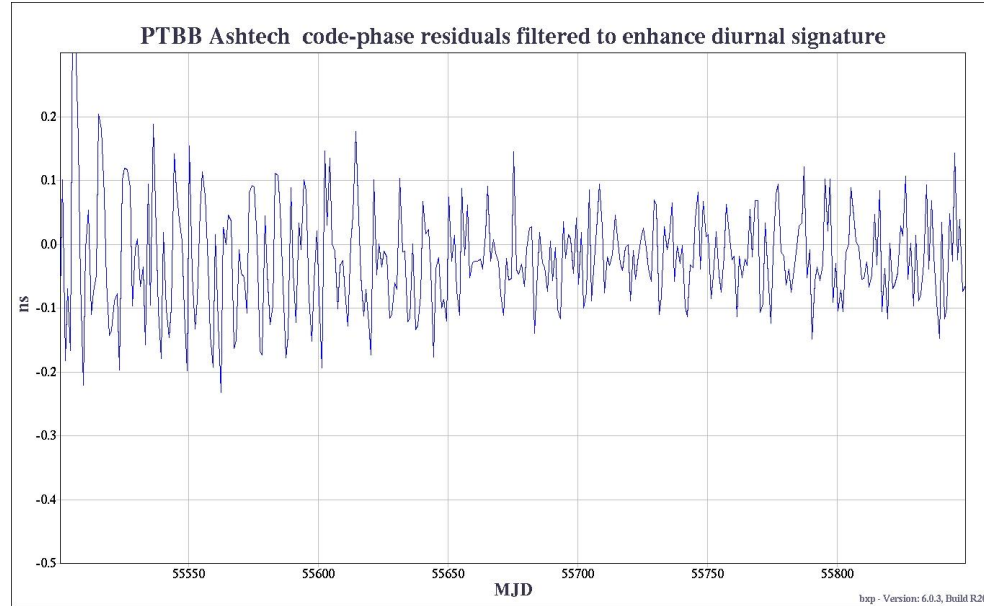


Figure 7. Code-Phase residuals from PTBB, an Ashtech receiver, filtered as described in Section 2.3 so that diurnals are mapped into a 10-day periodicity. Plots of the USNO's Ashtechs, whose IGS designations are USNO, USN3, and AMC2, are similar.

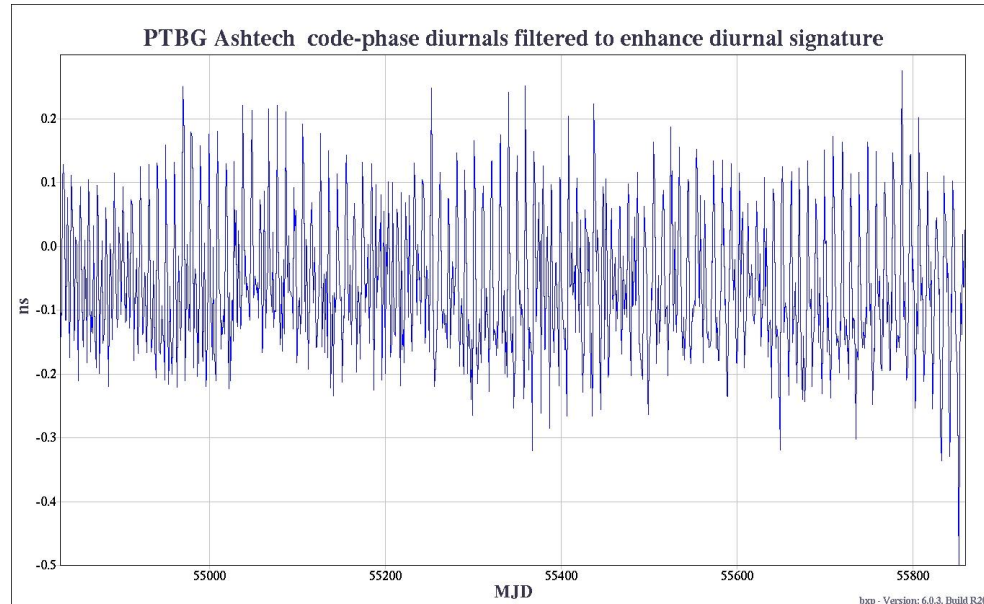


Figure 8. Code-Phase residuals of PTBG, filtered as described in Section 2.3 so that diurnals are mapped into a 10-day periodicity. Note that the diurnal variations are initially somewhat stronger than those of PTBB, and also persist through the summer.

3.3. NICT FOR A 22-MONTH PERIOD BETWEEN 0907-1104

Figure 9 illustrates a 22-month comparison between NICT2 and NICT for the period 0907 to 1104 using P3. Both receivers are Septentrio PolaRx2. The mean value of the differences and the standard deviation are 0.054 ns and ± 0.390 ns. The latter, together with its TDEV of 0.05 ns at an averaging time of 1 hour, proves that the short-term stability of the PolaRx2 is much better than that of the two Ashtech Z12T's at PTB. However, there appears to be a sinusoidal annual variation of 1.3 ns peak to peak in NICT2-NICT (B-A) between MJD 55120-55490. Figure 10 is a PPP reduction over the two receivers (A-B) over the last 20 months, and the difference with their third receiver that is under study (A-C). Receivers A and C have choke rings in their antennas. The latter appears to have instability in its P2 data [17].

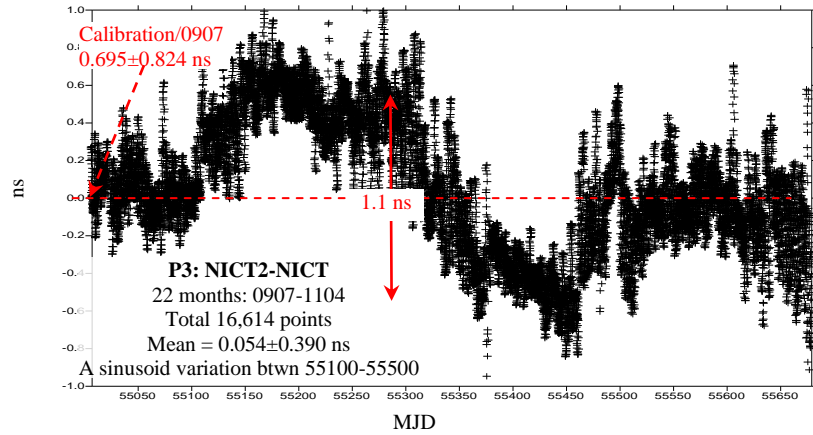


Figure 9. *Left:* Differences of NICT2-NICT vary between 0907–1104 with an apparently periodic variation, peak to peak 1.3 ns, about 1 year between MJD 55120-55490. Globally there would be a slight slope.

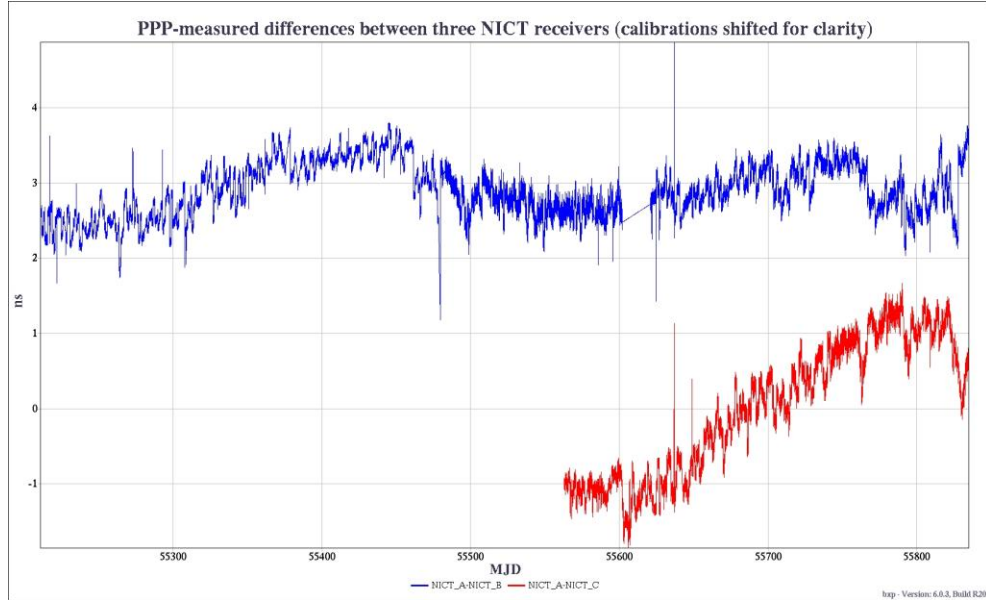


Figure 10. Differences between three receivers maintained at NICT (A-B). The lower curve is the common-clock difference between the operational unit and a newly received one that is under observation (A-C), which appears to have instability in its P2 data.

The code-phase residuals for the three receivers, shown below, reveal stronger diurnal signatures for receiver C and in the winter data for receiver A. By differencing code residuals from phase residuals we obtain Figures 11-13. As with the PTB receivers, the unit with the largest instability also shows the most pronounced code-phase signatures.

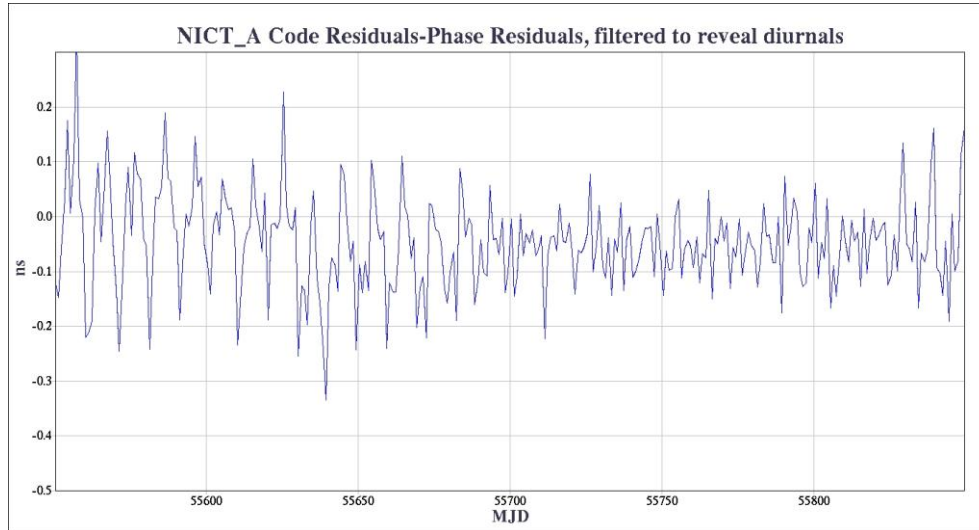


Figure 11. Differences between the code and the phase residuals of the receiver NICT A. Data are filtered as described in Section 2.3 so that diurnals are mapped into a 10-day periodicity.

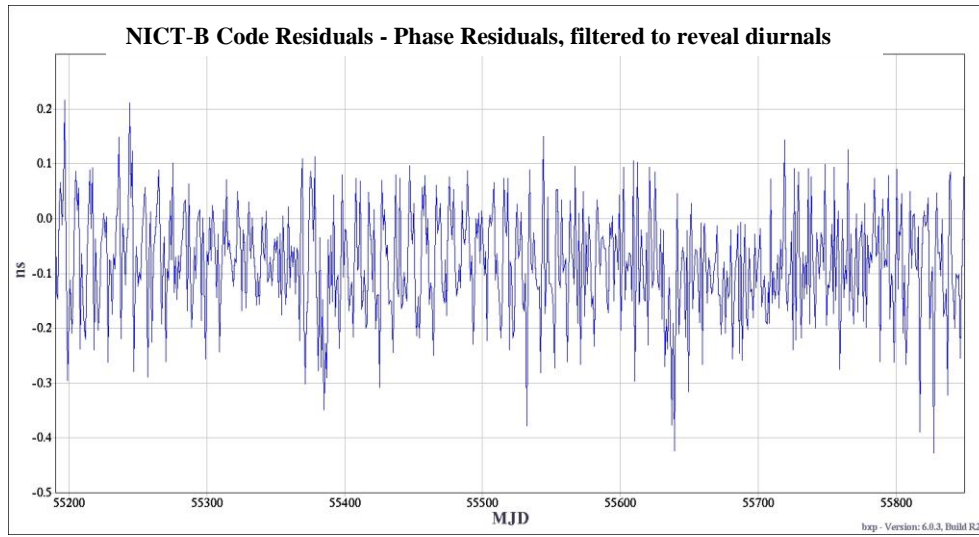


Figure 12. Differences between the code and the phase residuals of the receiver NICT B. Data are figured as described in Section 2.3 so that diurnals are mapped into a 10-day periodicity. Note that the variations do not decrease in the summer.

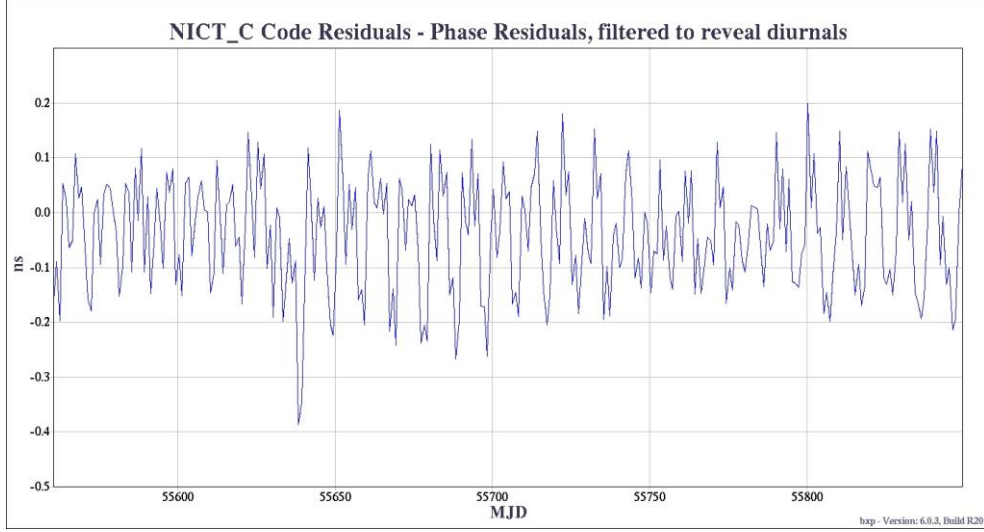


Figure 13. Differences between the code and the phase residuals of the receiver NICT C. Data are filtered as described in Section 2.3, so that diurnals are mapped into a 10-day periodicity. Note that the diurnals are stronger than in the other two receivers.

3.4. USNO RECEIVERS

The USNO observed a significant increase in the stability of its carrier-phase GPS receivers when they were moved to a room with higher temperature stability, although the situation is not yet optimal and the environmental conditions varied strongly when some of the data below were taken, due to improvements being made to the HVAC systems. Figure 14 shows the difference between the PPP solutions of two receivers over a 600-day period. To make this plot, the PPP solutions were forced to be continuous over several abrupt temperature variations in the room, and we suspect that the resulting 1.5 ns deviations would be significantly less if each receiver were in an individual chamber. Comparisons with other USNO receivers shows that the large variation from 55500-55600 was due to USN3. The data therefore suggest that both receivers would probably have subnanosecond stability if their temperature was kept constant to within 0.1 °C [16]. Figure 15 compares NOV1 with another modern receiver, and the deviations are less although kept in the same environment. It is interesting that the code-phase residuals of the NovAtel unit show a strong diurnal signature (Figure 16), although the data are among the most stable examined. The Septentrio unit showed a variable signature (Figure 17). Common-view analysis also showed subnanosecond consistency, but the details were slightly different from the USNO's PPP processing.

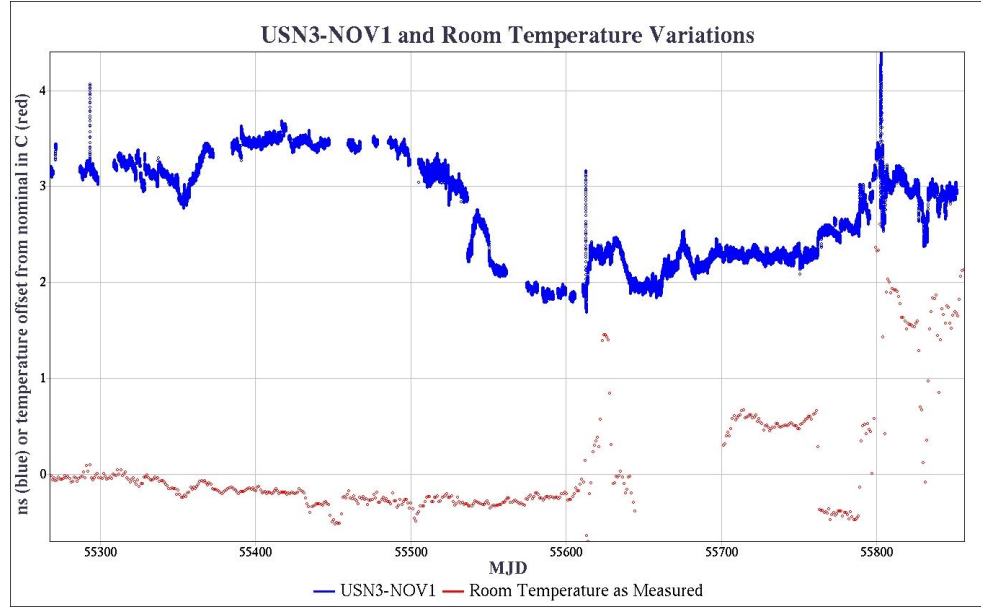


Figure 14. Difference between PPP solutions for two common-clock USNO receivers. Comparisons with other USNO receivers show that most of the variations are due to USN3, which can jump unpredictably due to environmental disturbances. Room variations were unusually high during this period, in part due to HVAC improvements. Curves are offset for display.

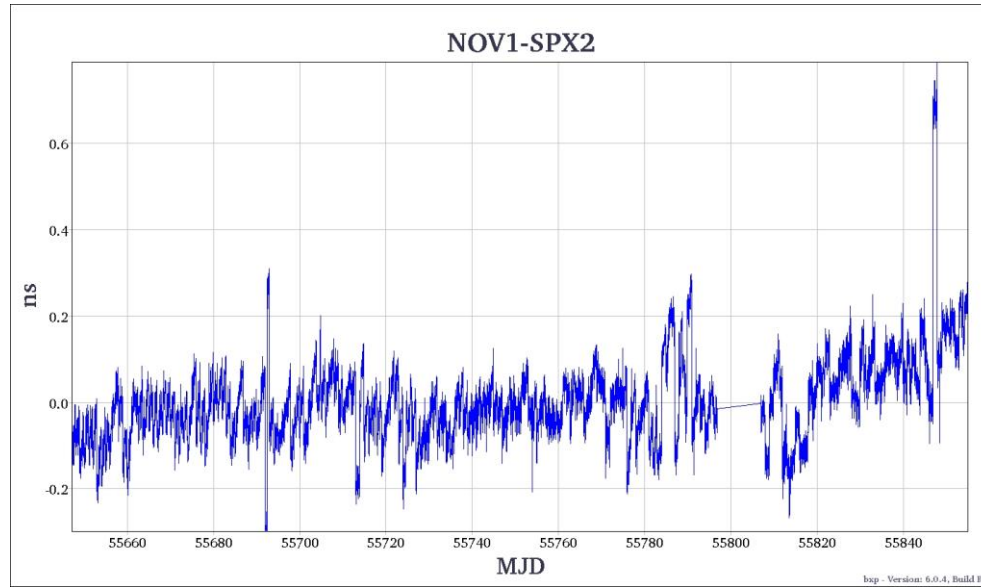


Figure 15. P3 between two 21st-century receivers maintained in the same room. Data were shifted due to a configuration change about MJD 55800.

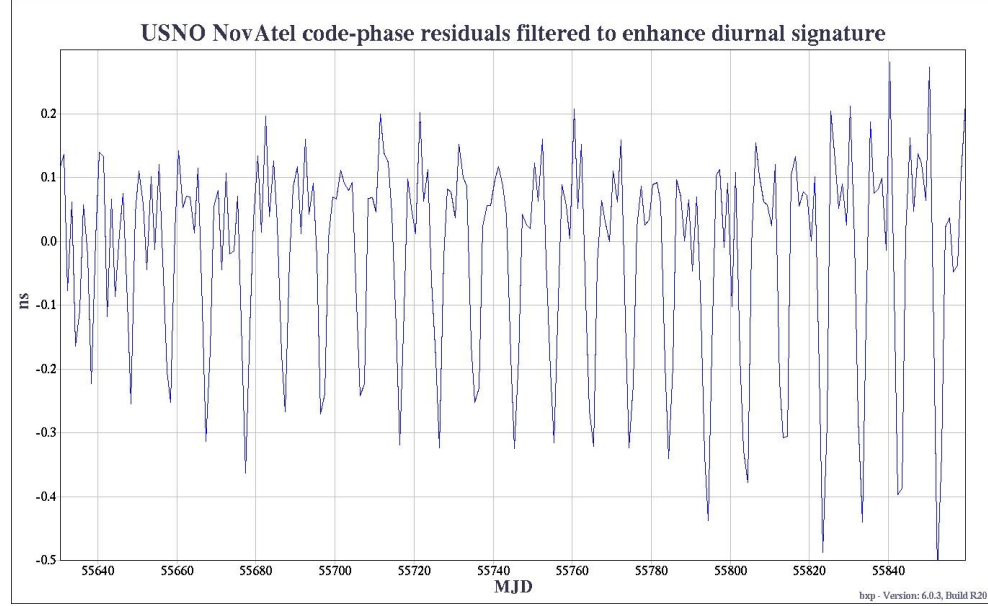


Figure 16. Code-phase residual data from the PPP solution of USNO's NovAtel receiver system, which are similar to those from NIST's NovAtel. The USNO's shares a common antenna with the Ashtech Z12T receiver USN3. Residuals are filtered as described in Section 2.3, so that diurnals are mapped into a 10-day periodicity.

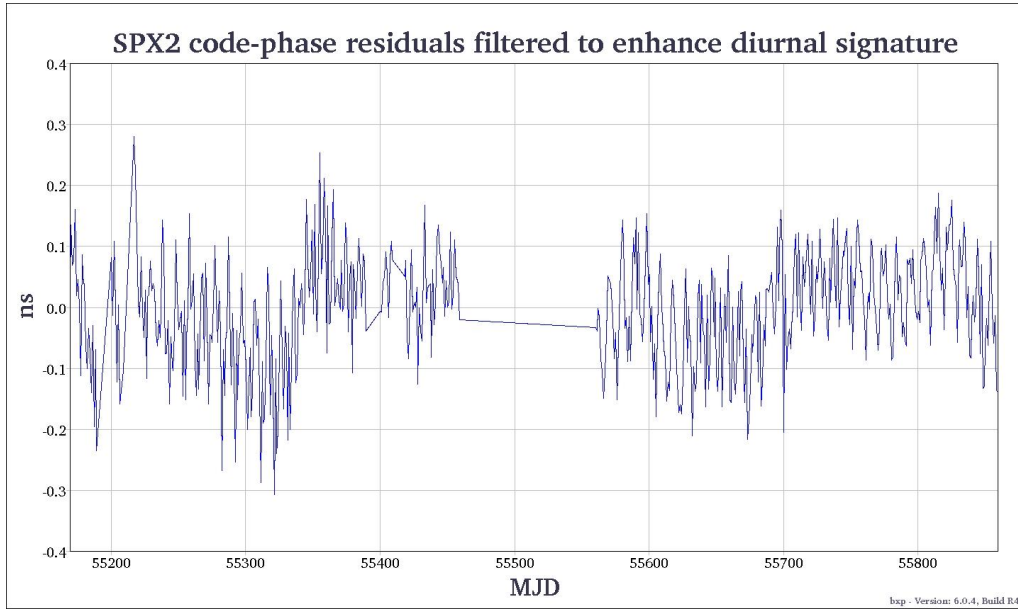


Figure 17. Code-phase residuals of SPX2. Data are filtered as described in Section 2.3, so that diurnals are mapped into a 10-day periodicity.

3.5. DISCUSSION OF THE RELATIVE VARIATION OF THE TOTAL SYSTEM DELAYS

(1) Jumps and long-term variations. While the 3 ns step in the CH01 receiver is due to an obvious environmental failure, other subnanosecond steps and the constant slopes may be caused by aging or more

subtle environmental events. We observed also some subnanosecond jumps, but even nanosecond jumps often go unnoticed and would be undetectable in laboratories with just one time-transfer system.

In monthly comparisons, it might be difficult to detect the long-term near-constant or zig-zag rates of between 1 ns and 2 ns per year found in Z12T/PTBG and Z12T/CH01 (Figures 2 and 5), or the sinusoidal annual variation seen in the pair of PolaRx2 (Figure 9). These variations may be related to environmental effects on the external parts of the receiver systems, such as the antenna and the cables.

(2) The Type B uncertainty. The receiver variation is not currently taken into account in the estimated calibration uncertainty (u_B). However, the BIPM considers that u_B increases with time since the calibration, and an analytical model based on an empirical value u_v has been proposed [8] as follows:

$$u_B^2(T - T_0)_{k\text{-PTB}} = u_B^2(T_0)_{k\text{-PTB}} + (T - T_0)(u_v)^2_{k\text{-PTB}}$$

Here $T - T_0$ is the time since the calibration and u_v is an empirical coefficient based on the above analysis of long-term variations of the receivers. As given in Table 2, for $u_v = 0.7 \text{ ns/month}^{1/2}$, the increase of u_B is 0.9 ns/year for the first year, and 0.7 ns/year for the second year, decreasing to 0.5 ns/year for the ninth year. This is, however, a first and phenomenological approach for an estimation of u_B , and must be discussed in detail and refined in future work. The values of u_B for different calibration ages are calculated on the basis of the above hypothesis and presented in Table 2. By 10 years u_B has increased to 10 ns, which in Circular T means the receiver is considered to be uncalibrated.

Table 2. Evolution of u_B increasing with age with different initial $u_B(T_0)$ and u_v for the UTC link (Lab_k-PTB).

Link	$u_B(T_0)$ /ns	u_v /(ns month ^{1/2})	$u_B(1\text{yr})$ /ns	$u_B(2\text{yr})$ /ns	$u_B(3\text{yr})$ /ns	$u_B(>10\text{yr})$ /ns
P code PPP	2.0	0.1	2.03	2.06	2.09	10
		0.4	2.4	2.8	3.1	10
		0.7	3.1	4.0	4.7	10
C/A & L1C codes	3.0	0.1	3.02	3.04	3.06	10
		0.4	3.3	3.6	3.8	10
		0.7	3.9	4.6	5.2	10

In [8], the equation was proposed under the reasoning that all links of a given type should be treated identically, and the Type B uncertainty should be large enough to cover receivers undergoing larger than usual and possibly unrecognized calibration variations outside the Gaussian assumption. We have observed more than one such situation in the course of this work. More important than the details of the expression used is that a steadily increasing uncertainty evaluation would have the effect of encouraging calibration efforts.

(3) An ensemble of GNSS receivers could provide a useful way of monitoring and, hence maintaining receiver calibrations, particularly with different models of receivers.

(4) We suggest that the UTC laboratories maintain redundant independent GNSS receivers to monitor the calibrations, and we note that the BIPM has requested data from redundant GNSS systems. Repeated absolute calibrations of a backup receiver and subsequent relative calibrations of the “working” receiver provide essential data on the long-term instability.

4. ACCURATE TIME TRANSFER WITH A DOUBLE-RECEIVER SYSTEM

The present strategy of UTC time transfer is single-receiver transfer. The above discussion demonstrates that the calibration reference of a receiver may suffer short-, middle-, and long-term instabilities at the nanosecond level. If these accumulate above a certain level, this could be a problem for UTC generation, particularly if the receiver in question is at the pivot laboratory, PTB. If one of the PTB receivers is biased, the part of the UTC network which is connected to PTB via this receiver will be biased with respect to the remaining laboratories. When the receiver of an individual laboratory is biased, the bias impacts UTC only through the link in question. As a first step towards understanding how an ensemble could be used, we study the case of a two-receiver set-up. Mathematically, we expect an improvement by a factor of $\sqrt{2}$ on all variations that are not common-mode. We note that receivers of the same make can respond differently even under the same temperature variations.

For this study, we combined the principal and backup P3 and PPP receivers of the PTB and CH, and data collected over 4 months from 1 January to 30 April 2011.

The method is straightforward: instead of using the measurement of a single receiver, we use the mean value of two receivers of each measurement epoch. All other computations and statistics follow the standard Circular T procedure using the BIPM software package Tsoft. We then investigate the smoothing residuals and the residuals compared to the GPS PPP solution, which is much more precise than the P3 solution and the time deviations.

Notation:

σ_1	Standard deviation of the Vondrak smoothing residuals
σ_2	Standard deviation of the differences between the link to study and the PPP link which is considered as a precise and independent reference
Lab	<i>Single</i> -receiver data
Lab ²	<i>Double</i> -receiver data; e.g., CH-PTB is a single-receiver link and CH ² -PTB ² is the double-receiver link; whereas CH-PTB ² and CH ² -PTB are single- and double-receiver mixed links.

4.1. COMPARISON OF THE STATISTICS

Table 3 and Table 4 show that for both of the above statistics, the standard deviations of the single-receiver link (CH-PTB) are greater than those of the single-double receiver link (CH-PTB²), which in turn are greater than those of the double-double receiver link (CH²-PTB²). If the instability of the receivers was characterized as white noise, an improvement of a factor of $\sqrt{2}$ would be expected. However the improvement, in particular in σ_2 , is significantly less than expected, which indicates that common biases exist in the P3 and PPP measurements, masking the white noise in P3. The gain of the double-receivers cannot be fully observed when taking PPP as reference.

Table 3. Comparison of the σ_1 for the baseline CH-PTB.

YYMM	$\sigma_1(\text{CH-PTB})$ /ns	$\sigma_1(\text{CH}^2\text{-PTB}^2)$ /ns	$\sigma_1(\text{CH-PTB}^2)$ /ns
1101	0.497	0.414	0.461
1102	0.463	0.400	0.436
1103	0.459	0.382	0.407
1104	0.469	0.401	0.428
Mean	0.465	0.399	0.433

Table 4. Comparison of the σ_2 for the baseline CH-PTB.

YYMM	$\sigma_2(\text{CH-PTB})$ /ns	$\sigma_2(\text{CH}^2\text{-PTB}^2)$ /ns	$\sigma_2(\text{CH-PTB}^2)$ /ns
1101	0.522	0.513	0.547
1102	0.502	0.461	0.479
1103	0.489	0.448	0.448
1104	0.496	0.476	0.468
Mean	0.502	0.474	0.492

4.2. COMPARISON OF THE TIME DEVIATIONS

In this section, we compare time instabilities of the links computed with the classical P3 single-receiver AV method and the double-receiver method. Figures 18 and 19 illustrate the TDEV of the baseline CH-PTB for different averaging times: 1 month and 4 months. The time links are those of the receiver pairs of single-single, double-double, and single-double. Generally speaking, the double-receiver links are better than the single-receiver links. As discussed in Sections 3.2 and 3.5, the receiver pair at PTB is noisier than that at CH. Therefore, the double-receivers at PTB give an immediate improvement, as shown in the plots CH-PTB² in the figures. This is supported by the statistics given in the Tables 3 and 4. In particular, for an averaging time of about 12 h, CH-PTB² gives the best stability. On the other hand, the time stability for averaging times of more than 1 day is not significantly improved. This is of particular importance, because in the current scheme the computation of UTC yields a time-scale difference only every 5 days. It is, thus, possible to improve the short-term stability of all UTC time links through a rather simple effort to improve the receiver stability at PTB. PTB has started to provide GPS data (RINEX and CGGTTS) from a Dicom GTR50 receiver and just started to operate a Septentrio PolaRx4, which will in the future provide GPS, GLONASS, and Galileo observation data.

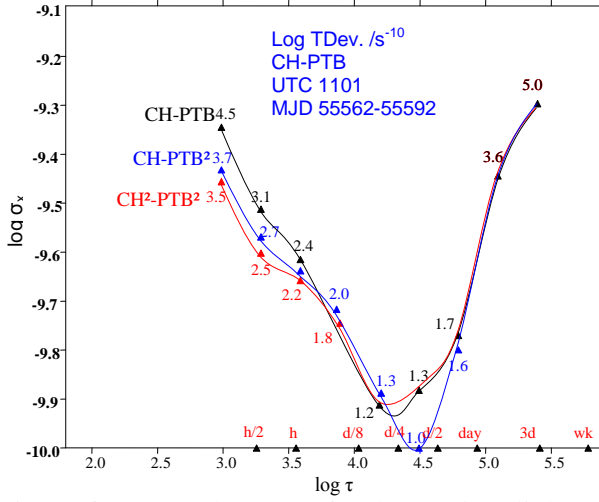


Figure 18. Comparison of a 1-month TDEV for the P3 time link CH-PTB of UTC1103 (N=745).

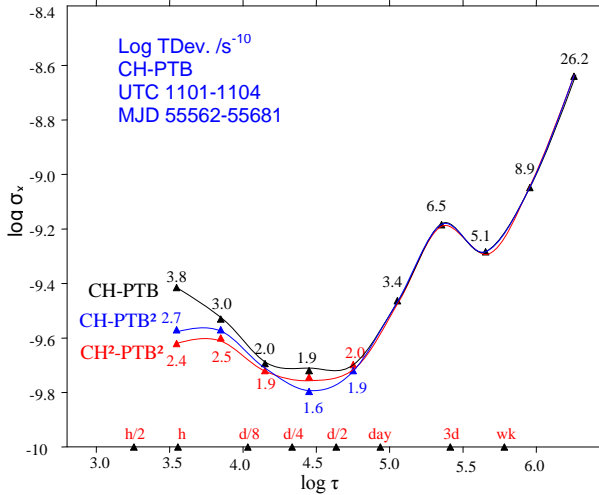


Figure 19. TDEV comparison of a 4-month P3 time link to PPP for CH-PTB of UTC1101-1104 (N=2948).

5. SUMMARY

By a common-clock, short-baseline(s) analysis of data from CH, NICT, PTB, and USNO, we have confirmed that long-term variations of between 1 ns and 2 ns per year are common for 20th-century receivers, while smaller variations have been seen in newer units. This is not surprising, as some GPS receiver models used in timing applications today were initially intended for geodetic applications in which the internal delays matter to a lesser extent due to the common practice of double-differencing the observations. In view of this, METAS had in the 1990s designed its GeTT terminal with a thermally stabilized enclosure for the geodetic GPS receiver [16]. In certain situations, the receiver variations can accumulate to form much larger offsets, and this emphasizes the need for frequent calibrations. These findings support the suggestion that the estimated calibration uncertainty of a link at a certain epoch should be increased as it is extrapolated over extended periods.

We conclude that GNSS receiver ensembles could be used to identify (and subsequently eliminate) spontaneous receiver jumps at the subnanosecond level, along with information such as environmental failures or installation modifications.

An ensemble of GNSS receivers operated in one laboratory will facilitate further studies, and detailed records may be useful for receiver manufacturers. Combining the results will reduce the influence of individual devices, assuming that each varies independently of its neighbors. We have investigated the double-receiver time transfer and shown that the use of a second time transfer system may improve the link stability with regard to jumps, measurement noise, and long-term variations. We note that our use of the term “receiver” includes all components of the system, and that in some cases the comparison to existing and completely independent TWSTFT links would also help to identify individual receiver instabilities. The use of an ensemble would provide a useful supplement to the BIPM’s standard calibrations via a traveling GNSS calibration device, both as a check of accuracy and as a means of determining which laboratories are most in need of calibration.

Finally, the calibration variation of a GNSS receiver system depends on the long-term stability of the code data. We will continue to investigate variations in the C/A, L1C, and P codes, in particular due to non-environmental effects such as material or electronic aging. The independent technique TWSTFT is helpful for this. We encourage the laboratories that operate redundant receivers and/or systems to routinely monitor the stability of their equipment. The BIPM is developing a standard CGGTTS code-based, common-clock CV comparison procedure to continuously check the stabilities of the equipment. The BIPM has published monthly comparisons since 2005, and long-term comparisons between TWSTFT, GPS, and GLN for UTC or certain non-UTC baselines since 2008 [18]. The results are available on <ftp://tai.bipm.org/TimeLink/LkC/>, and are intended to be an aid to the UTC laboratories. We also suggest that time laboratories operate a backup receiver, study the performance of receiver types, and document the results in a systematic way to identify which receiver or receiver type is particularly stable, and that more frequent receiver calibrations through the BIPM or the CIPM MRA should be organized.

DISCLAIMER

Although some manufacturers are identified for the purpose of scientific clarity, the authors do not endorse any commercial product, nor do we permit any use of this document for marketing or advertising. We further caution the reader that the equipment quality described here may not be characteristic of similar equipment maintained at other laboratories, nor of equipment currently marketed by any commercial vendor. In this work, many of the effects associated with a GPS receiver’s system may be due to equipment supplying signals to the GPS receiver.

REFERENCES

- [1] W. Lewandowski, D. N. Matsakis, G. Panfilo, and P. Tavella, 2005, “*First Evaluation And Experimental Results On the Determination of the Uncertainties in UTC-UTC(k)*,” in Proceedings of the 36th Annual Precise Time and Time Interval (PTTI) Systems and Applications Meeting, 7-9 December 2004, Washington, D.C., USA (U.S. Naval Observatory, Washington, D.C.), pp. 247-261.
- [2] W. Lewandowski, D. N. Matsakis, G. Panfilo, and P. Tavella, 2005, “*On the Evaluation of the Uncertainties in UTC-UTC(k)*,” in Proceedings of the 19th European Time and Frequency Forum (EFTF), 21-24 March 2005, Besançon, France, p. 83.

- [3] D. N. Matsakis, K. Senior, and P. Cook, 2002, “*Comparison of Continuously Filtered GPS Carrier Phase Time and Frequency Transfer with Independent Daily GPS Carrier Phase Solutions and with Two-Way Satellite Time Transfer*,” in Proceedings of the 33th Annual Precise Time and Time Interval (PTTI) Systems and Applications Meeting, 27-29 December 2001, Long Beach, California, USA (U.S. Naval Observatory, Washington, D.C.), pp. 63-88.
- [4] D. N. Matsakis, 2011, “*Time and Frequency Activities of the USNO*,” in Proceedings of the 42nd Annual Precise Time and Time Interval (PTTI) Systems and Applications Meeting, 16-18 November 2010, Reston, Virginia, USA (U.S. Naval Observatory, Washington, D.C.), pp. 11-32.
- [5] D. N. Matsakis, 2010, “*USNO Station Report*,” 19th Meeting of the CCTF Working Group on TWSTFT, http://www.bipm.org/wg/CCTF/TWSTFT/Allowed/WG_19th_Meeting/19-06-2_USNO_stationreport.twstt.2011.pdf
- [6] F. Arias and Z. Jiang, 2008, “*Considerations on unifying the TWSTFT and GPS Calibration for UTC time transfer*,” 16th Meeting of the CCTF Working Group on TWSTFT, 2-3 October 2008, SP, Boras, Sweden.
- [7] M. Weiss, V. Zhang, J. White, K. Senior, D. Matsakis, S. Mitchell, P. Uhrich, D. Valat, W. Lewandowski, G. Petit, A. Bauch, T. Feldmann, and A. Proia, 2011, “*Coordinating GPS Calibrations among NIST, NRL, USNO, PTB and OP*,” in Proceedings of the IEEE International Frequency Control Symposium and European Frequency and Time Forum (EFTF) Joint Conference, 2-5 May 2011, San Francisco, California, USA (IEEE), pp. 1070-1075.
- [8] Z. Jiang, G. Petit, F. Arias, and W. Lewandowski, 2011, “*BIPM Calibration Scheme for UTC Time Links*,” in Proceedings of the IEEE International Frequency Control Symposium and European Frequency and Time Forum (EFTF) Joint Conference, 2-5 May 2011, San Francisco, California, USA (IEEE), pp. 1064-1069.
- [9] D. Piester, A. Bauch, L. Breakiron, D. Matsakis, B. Blanzano, and O. Koudelka, 2008, “*Time transfer with nanosecond accuracy for the realization of International Atomic Time*,” **Metrologia**, **45**, 185-192.
- [10] A. Bauch, D. Piester, B. Blanzano, O. Koudelka, E. Kroon, E. Dierikx, P. Whibberley, J. Achkar, D. Rovera, L. Lorini, F. Cordara, and C. Schlunegger, 2009, “*Results of the 2008 TWSTFT Calibration of Seven European Stations*,” in Proceedings of the European Frequency and Time Forum (EFTF), 21-24 April 2009, Besançon, France, pp. 1209-1215.
- [11] D. N. Matsakis, M. Lee, R. Dach, U. Hungentobler, and Z. Jiang, 2006, “*GPS Carrier Phase Analysis Noise on the USNO-PTB Baselines*,” in Proceedings of the IEEE International Frequency Control Symposium, 5-7 June 2006, Miami, Florida, USA (IEEE 06CH37752), pp. 631-636.
- [12] L. A. Breakiron, 2011, “*The Stability of GPS Carrier-Phase Receivers*,” in Proceedings of the 42nd Precise Time and Time Interval (PTTI) Systems and Applications Meeting, 15-18 November 2010, Reston, Virginia, USA (U.S. Naval Observatory, Washington, D.C.), pp. 295-304.
- [13] T. Feldmann, A. Bauch, D. Piester, A. Stefanov, L.-G. Bernier, C. Schlunegger, and K. Liang, 2010, “*On Improved GPS Based Calibration of the Time Links Between METAS and PTB*,” in Proceedings of the 24th European Frequency and Time Forum (EFTF), 13-16 April 2010, Noordwijk, The Netherlands, paper 12.3.

- [14] N. Guyennon, G. Cerretto, P. Tavella, and F. Lahaye, 2009, “*Further Characterization of the Time Transfer Capabilities of Precise Point Positioning (PPP): the Sliding Batch Procedure,*” **IEEE Transactions on Ultrasonics, Ferroelectrics, and Frequency Control**, UFFC-56, 1634-1641.
- [15] L. G. Bernier, 2011, “*Thernam control failure CH01-WAB2,*” METAS Internal Report RT919993201.
- [16] G. Dudle, F. Overney, L. Prost, T. Schildknecht, and T. Springer, 1999, “*First Results on a Transatlantic Time and Frequency Transfer by GPS Carrier Phase,*” in Proceedings of the 30th Precise Time and Time Interval (PTTI) Systems and Applications Meeting, 1-3 December 1998, Reston, Virginia, USA (U.S. Naval Observatory, Washington, D.C.), pp. 271-280.
- [17] Gotoh Tadahiro, 2011, e-mail communication.
- [18] E. F. Arias, Z. Jiang, G. Petit, and W. Lewandowski, 2005, “*BIPM Comparison of Time Transfer Techniques,*” in Proceedings of the 2005 Joint IEEE International Frequency Control Symposium and Precise Time and Time Interval (PTTI) Systems and Applications Meeting, 29-31 August 2005, Vancouver, Canada (IEEE 05CH37664C), pp 312-315.